Langmuir

Article

pubs.acs.org/Langmuir

Effects of Salting-In Interactions on Macromolecule Diffusiophoresis and Salt Osmotic Diffusion

Michele S. McAfee and Onofrio Annunziata*

Department of Chemistry, Texas Christian University, Fort Worth, Texas 76129, United States

Supporting Information

ABSTRACT: Macromolecule diffusiophoresis (i.e., macromolecule migration induced by a salt concentration gradient) in water and salt osmotic diffusion (i.e., salt migration induced by a macromolecule concentration gradient) are two cross-diffusion mechanisms caused by macromolecule−salt interactions. We investigated the effect of salting-in interactions on the behavior of these two cross-diffusion mechanisms. Our results are distinct from those previously obtained in the case of salting-out interactions. Cross-diffusion was experimentally characterized by Rayleigh interferometry at 25 °C. Specifically, multicomponent diffusion coefficients were measured for a neutral polymer, polyethylene glycol (molar mass, 20 kg/mol), in aqueous solutions of three thiocyanate salts (NaSCN, KSCN, and NH_4SCN) as a function of salt concentration at low polymer concentration (0.5% w/w). Our results on salt osmotic diffusion, which were qualitatively different from those previously obtained for salting-out salts, were used to quantitatively characterize the strength of salting-in interactions. The behavior of polymer diffusiophoresis as a function of salt concentration and cation type reveals that polymer chains have an extrinsic negative charge, consistent with anion binding being the cause of salting-in interactions. To quantitatively examine the effect of anion binding on salt osmotic diffusion and polymer diffusiophoresis, we developed a theoretical model based on the linear laws of nonequilibrium thermodynamics for diffusion, the Scatchard binding model, and particle electrophoresis. This work contributes to the understanding of the multifaceted effects of molecular interactions on cross-diffusion mechanisms, salting-in interactions, and the Hofmeister series.

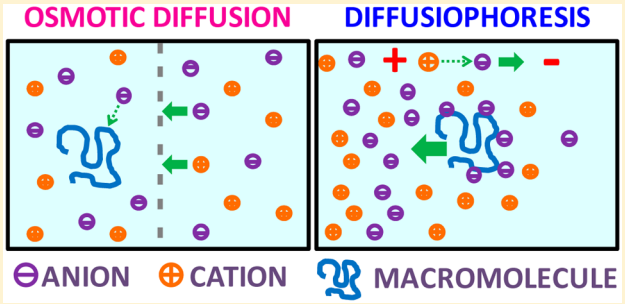

1. INTRODUCTION

The effect of salts on the thermodynamic properties of macromolecular aqueous solutions has been extensively investigated. In many studies, inorganic anions have been ranked according to their salting-out strength, that is, their effectiveness in precipitating proteins and synthetic polymers, leading to the well-known Hofmeister series.[1−8] In this series, anions such as SO_4^{2-} display a great salting-out strength, whereas Cl^- is regarded as a neutral anion located approximately at the midpoint of the Hofmeister series, separating salting-out from salting-in anions such as SCN^-, which increase the solubility of macromolecules in water.[5,6] These effects have been historically attributed to ion−water interactions; that is, they were associated with the influence of anions on the hydrogen-bonding network of bulk water. Specifically, salting-out anions are water structure makers (kosmotropes), whereas salting-in anions are water structure breakers (chaotropes). However, recent studies revealed that macromolecule−ion interactions are the main factor responsible for changes in macromolecule solubility in water. This implies that the mechanism of action of salting-in anions is better described as the binding of anions to macromolecules.[8−10]

Compared to anions, the Hofmeister series for cations is significantly less pronounced, and the cation ranking can depend on the chemical nature of the macromolecule investigated. The most common cations, Na^+ and K^+, exhibit salting-out properties. Another familiar cation, NH_4^+, is usually positioned at greater salting-out strength. Nevertheless, several studies have also shown that NH_4^+ displays a salting-out strength weaker than those of both Na^+ and K^+.[4−6]

Salts also affect the transport properties of macromolecule aqueous solutions. This becomes particularly interesting when considering multicomponent diffusive transport, especially in relation to the cross-diffusion phenomenon caused by macromolecule−salt interactions.[11−13] For a ternary macromolecule (1)−salt (2)−water (0) system, multicomponent diffusion can be described by the extended Fick's first law[11,14]

$$-J_1 = D_{11}\nabla C_1 + D_{12}\nabla C_2 \quad (1a)$$

$$-J_2 = D_{21}\nabla C_1 + D_{22}\nabla C_2 \quad (1b)$$

where C_1 and C_2 are the molar concentrations of macromolecule and additive, respectively; J_1 and J_2 are the corresponding molar fluxes; and the four D_{ij} values (with $i, j = 1, 2$) are the multicomponent diffusion coefficients (usually

Received: November 26, 2014
Revised: January 8, 2015
Published: January 10, 2015

DOI: 10.1021/la5046223
Langmuir 2015, 31, 1353−1361

described in volume- or solvent-fixed reference frames).[14] Diffusion coefficients D_{11} and D_{22}, which characterize the fluxes of polymer and salt due to their own concentration gradients, describe normal diffusion of these two solute components. On the other hand, D_{12} and D_{21}, which characterize the flux of a solute due to the concentration gradient of the other solute, describe the phenomenon of cross-diffusion. To distinguish between the two cross-diffusion coefficients, we denote D_{12} and D_{21} as the coefficients of macromolecule diffusiophoresis and salt osmotic diffusion, respectively.[11]

Salt-induced diffusiophoresis of colloidal particles has attracted much attention because the manipulation of particle motion by salt concentration gradients can be exploited for applications in self-assembly and adsorption processes.[15−19] Nearly all studies on salt-induced diffusiophoresis have been limited to the case of large (∼100 nm) particles in the presence of aqueous chloride salts (e.g., NaCl and KCl) at low salt concentrations (∼0.1 mol·dm^{-3} or less). Under these conditions, electrostatic ionic interactions dominate. Recently, we showed that salt-induced diffusiophoresis can also be observed in the case of macromolecules such as proteins and neutral polymers.[11−13] These studies, which were extended to salt concentrations as a high as ∼2 mol·dm^{-3}, allowed for an examination of how the magnitude of macromolecule diffusiophoresis is related to macromolecule−salt specific interactions in water. Moreover, salt osmotic diffusion was also characterized and exploited to determine macromolecule preferential-hydration parameters, which characterize macromolecule−salt thermodynamic interactions in water. In two recent studies,[12,13] we characterized polymer diffusiophoresis and salt osmotic diffusion for polyethylene glycol (PEG), a biocompatible synthetic macromolecule extensively employed in pharmaceutical and industrial applications.[20,21] Because PEG is a hydrophilic neutral polymer, hydration effects become the dominant source of salt-induced polymer diffusiophoresis. This aspect allowed us to experimentally characterize PEG diffusiophoresis in the presence of salting-out salts. Specifically, we employed precision Rayleigh interferometry[22] to experimentally determine the four ternary diffusion coefficients in aqueous salt solutions of PEG (molar mass of 20 kg mol^{-1}) of chloride and sulfate salts at 25 °C. Our results showed that the magnitude of PEG diffusiophoresis significantly increases when mild salting-out agents such as NaCl are replaced by strong ones such as Na_2SO_4. Preferential-hydration parameters, which were extracted from related results on salt osmotic diffusion, allowed the ranking of both anions (SO_4^{2-} > Cl^-) and cations (Na^+ > K^+ > Ca^{2+} > NH_4^+) with respect to their salting-out effectiveness on PEG.[13] These rankings were consistent with the Hofmeister series. Our findings also showed that diffusiophoresis of macromolecules can be exploited in diffusion-based mass-transfer processes. For example, salt concentration gradients could be used to design and control the self-assembly and crystallization of macromolecules near a membrane or facilitate the adsorption of macromolecules on solid supports positioned near this membrane.[12,13]

To our knowledge, experimental studies on salt-induced particle diffusiophoresis or salt osmotic diffusion relative to salting-in salts have not previously been reported. Thus, in this work, we applied precision Rayleigh interferometry to experimentally determine PEG diffusiophoresis and salt osmotic diffusion in the cases of NaSCN, KSCN, and NH_4SCN at 25 °C. Our results were compared with those previously obtained for NaCl, KCl, and NH_4Cl under the same experimental conditions. The observed behavior of salt osmotic diffusion was utilized to quantitatively characterize the salting-in strengths of these three thiocyanate salts, whereas our theoretical examination of polymer diffusiophoresis allowed us to associate salting-in interactions with anion binding.

2. EXPERIMENTAL SECTION

2.1. Materials. Poly(ethylene glycol) (PEG) with a nominal molar mass of 20 kg mol^{-1} was purchased from Sigma-Aldrich and used without further purification. For PEG, certificates of analysis obtained from Sigma-Aldrich gave the number- (M_n) and mass- (M_w) average molar masses based on size-exclusion chromatography: M_n = 18.0 kg·mol^{-1} and M_w/M_n = 1.37 for lot 1120242 (PEG lot A) and M_n =24.0 kg·mol^{-1} and M_w/M_n = 1.05 for lot BCBG0180 V (PEG lot B). NaSCN (purity, 99.9%; molar mass, 81.07 g·mol^{-1}), KSCN (purity, 100.0%; molar mass, 97.18 g·mol^{-1}), and NH_4SCN (purity, 99.1%; molar mass, 76.12 g·mol^{-1}) were obtained from Sigma-Aldrich and used without further purification. Deionized water was passed through a four-stage Millipore filter system to provide high-purity water for all experiments. Stock concentrated aqueous binary solutions of PEG, NaSCN, KSCN, and NH_4SCN were made by weight to 0.1 mg and then filtered (0.2-μm pore size). Stock solutions (10−50% w/w) were prepared by mixing at least 30 g of solute with water. Density measurements (Mettler-Paar DMA40 density meter) were performed on the stock solutions for buoyancy corrections. All solutions for Rayleigh interferometry were prepared by mass. For binary PEG−water and salt−water experiments, precise masses of stock solutions were diluted with pure water to reach the final target concentrations. For ternary PEG−salt−water solutions, precise masses of PEG and salt stock solutions were added to flasks and diluted with pure water to reach the final target PEG and salt concentrations. The densities of these solutions were measured (with a precision of $\pm 2 \times 10^{-5}$ g·cm^{-3} or better) to determine partial molar volumes (with a precision of ∼0.5%) and molar concentrations of polymer and salt. Polymer molar concentrations were based on a molar mass of 20 kg mol^{-1}.

2.2. Rayleigh Interferometry. Binary and ternary mutual diffusion coefficients were measured at 25.00 °C with the Gosting diffusiometer operating in Rayleigh interferometric optical mode.[23] The refractive-index profile inside a diffusion cell was measured as described in ref 22 and references therein to obtain the diffusion coefficients in the volume-fixed reference frame.[24] A minimum of two experiments is required for determining the four diffusion coefficients at a given set of mean concentrations of polymer (C_1, mol·dm^{-3}) and salt (C_2, mol·dm^{-3}). These two experiments must have different combinations of solute concentration differences across the diffusion boundary. To verify reproducibility, two other duplicate experiments were performed at each set of mean concentrations. The four ternary diffusion coefficients, D_{ij}, were obtained by applying the method of nonlinear least squares as described in ref 25. Because of the PEG molar-mass polydispersity, a corrective procedure was applied to our ternary experiments to remove the contribution of polydispersity from the measured refractive-index profiles. This procedure, which is based on the refractive-index profiles of the corresponding binary PEG−water experiments, is described in ref 26 in detail.

3. RESULTS AND DISCUSSION

For the three thiocyanate salts investigated, the four multicomponent diffusion coefficients, D_{ij}, were obtained at a PEG concentration of $C_1 = 0.25 \times 10^{-3}$ mol·dm^{-3} (5.0 g·dm^{-3}) as a function of salt concentration, C_2, up to 2 mol·dm^{-3}. These data are available in the Supporting Information. To examine D_{12} and D_{21}, it is convenient to consider these two normalized cross-diffusion coefficients[12,13]

$$\hat{D}_{12} \equiv \lim_{C_1 \to 0} \left(\frac{D_{12}}{C_1} + \frac{\bar{V}_2 D_2}{1 - C_2 \bar{V}_2} \right) \frac{C_2}{\nu_2 y_2 D_1^0} \tag{2a}$$

DOI: 10.1021/la5046223
Langmuir 2015, 31, 1353−1361

$$\hat{D}_{21} \equiv \lim_{C_1 \to 0} (D_{21} + C_2 \bar{V}_1 D_1^0) \frac{1}{D_2} \tag{2b}$$

where $\bar{V}_2$ is the salt partial molar volume and $y_2 \equiv 1 + (\mathrm{d} \ln f_2)/(\mathrm{d} \ln C_2)$, with f_2 being the salt mean-ionic activity coefficient, is the nonideality thermodynamic factor. Because experimental diffusion coefficients are measured in the volume-fixed frame, the second term within parentheses in eqs 2a and 2b represents a correction needed to convert cross-diffusion coefficients from the volume-fixed to the solvent-fixed frame. Note that the binary salt diffusion coefficient, D_2 in eqs 2a and 2b, is defined with respect to the volume-fixed frame, whereas D_1^0, being a tracer-diffusion coefficient, is independent of the reference frame employed. The coefficient ν_2 in eq 2a describes electrolyte dissociation ($\nu_2 = 2$ for all three salts investigated). Because the experimental polymer concentration is fairly low, the measured values of D_{12} and D_{21}, together with the other available[27,28] physicochemical properties (see Supporting Information) shown in eqs 2a and 2b, can be directly used to calculate the normalized cross-diffusion coefficients, $\hat{D}_{12}$ and $\hat{D}_{21}$, within the experimental error of cross-diffusion coefficients. Values of D_1^0 as a function of salt concentration were obtained by using the relation $D_1^0(C_2) = D_1^0(0)/\eta_r(C_2)$, where $D_1^0(0)$ is the polymer tracer-diffusion coefficient in water[12] and $\eta_r(C_2)$ is the relative viscosity of the corresponding binary salt–water system.[27,28] More details on the physical meanings of these two normalized coefficients are discussed in refs 11–13.

3.1. Salt Osmotic Diffusion. We start by examining the behavior of $\hat{D}_{21}(C_2)$, due to its association with thermodynamic interactions. In Figure 1, we plot $\hat{D}_{21}$ as a function of salt concentration for all three thiocyanate salts together with previously obtained experimental results for the corresponding chloride salts.[13] Note that $\hat{D}_{21}$ must approach zero as $C_2 \to 0$. The baseline, namely, $\hat{D}_{21} = \bar{V}_1 C_2$ with $\bar{V}_1 = 16.7$ dm^3·mol^{-1}, is included (dotted line) in Figure 1 for comparison; it represents the nonspecific excluded-volume contribution of bare polymer chains to $\hat{D}_{21}$.[13] Positive or negative deviations of $\hat{D}_{21}(C_2)$ from this baseline characterize the strength of repulsive (salting-out) or attractive (salting-in) polymer–salt thermodynamic interactions, respectively. As one can see in Figure 1, the behavior observed for chloride salts is consistent with salting-out interactions. On the other hand, the $\hat{D}_{21}(C_2)$ curves associated with the thiocyanate salts are located below the baseline and are convex downward. In the case of NH_4SCN, the $\hat{D}_{21}(C_2)$ curvature is so strong that $\hat{D}_{21}(C_2)$ is negative at low C_2, exhibits a minimum at $C_2 \approx 0.5$ mol·dm^{-3}, and then becomes positive for $C_2 > 1$ mol·dm^{-3}. For both chloride and thiocyanate salts, the magnitude of $\hat{D}_{21}(C_2)$ follows the order $Na^+ > K^+ > NH_4^+$, which characterizes the relative salting-out strengths of these cations. However, the differences among cations are relatively large in the case of thiocyanates when compared to those observed for chlorides.

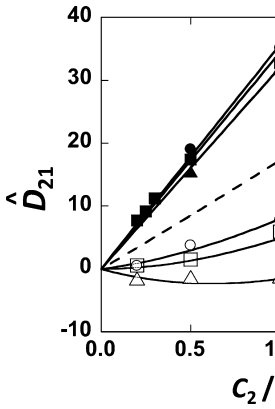

Figure 1. Normalized cross-diffusion coefficient, $\hat{D}_{21}$, as a function of salt concentration, C_2, describing salt osmotic diffusion for NaSCN (○), KCSCN (□), and NH_4SCN (△); NaCl (●), KCl (■), and NH_4Cl (▲). For the chloride salts, the solid lines are linear fits through the data. For the thiocyanate salts, solid curves are generated by applying the ligand model (eqs 4 and 7) to eqs 3a and 3b. The dashed line represents $\hat{D}_{21} = \bar{V}_1 C_2$.

The behavior of $\hat{D}_{21}(C_2)$ obtained in the case of thiocyanate salts can be explained by considering the binding of SCN^- anions to PEG chains. The observed curvatures in Figure 1 can be related to the saturation of the binding sites on the polymer chain. In other words, PEG–salt attractive interactions become weaker as the salt concentration increases toward the saturation of the polymer binding sites. This leads to a corresponding reduction of the negative deviations of the $\hat{D}_{21}(C_2)$ curves from the baseline.

Because the mobility of polymer chains is significantly lower than that of small ions,[13] the effect of ion binding on salt osmotic diffusion can be described by considering the equilibrium-dialysis scheme shown in Figure 2. Here, two compartments containing a ternary polymer–salt–water system and a binary salt–water system are in chemical equilibrium with respect to the salt component through a membrane that is not permeable to macromolecules. Anion binding reduces the concentration of free ions in the ternary compartment, thereby promoting salt osmotic diffusion from the binary to the ternary compartment. This mechanism leads to a negative contribution to the net value of $\hat{D}_{21}$, consistent with our results in Figure 1.

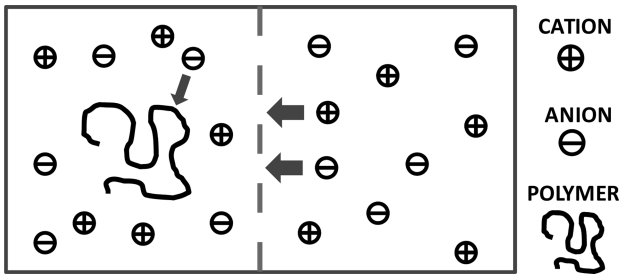

Figure 2. Equilibrium-dialysis scheme in which a polymer–salt–water compartment (left) is in equilibrium with a salt–water compartment through a membrane (vertical dashed line) that is not permeable to the polymer. The binding of the anion to the polymer leads to the osmotic diffusion of the cation and anion from right to left ($\hat{D}_{21} < 0$). The same effect will occur for cation binding.

3.2. Polymer Diffusiophoresis. Although our experimental results on salt osmotic diffusion allow us to probe salting-in interactions, the behavior of salt osmotic diffusion alone is not necessarily caused by an actual binding of anions to PEG. Other salting-in mechanisms such as changes in water H-bond structure or even cation binding can potentially be proposed to qualitatively explain our $\hat{D}_{21}(C_2)$ results. Indeed, our proposed anion-binding mechanism is guided by previous studies[8–10] on other macromolecules. We will now show that the experimental behavior of the other normalized cross-diffusion coefficient, $\hat{D}_{12}(C_2)$, reflects anion binding.

DOI: 10.1021/la5046223
Langmuir 2015, 31, 1353–1361

In Figure 3, we plot $\hat{D}_{12}$ as a function of salt concentration for all three thiocyanate salts together with previously obtained

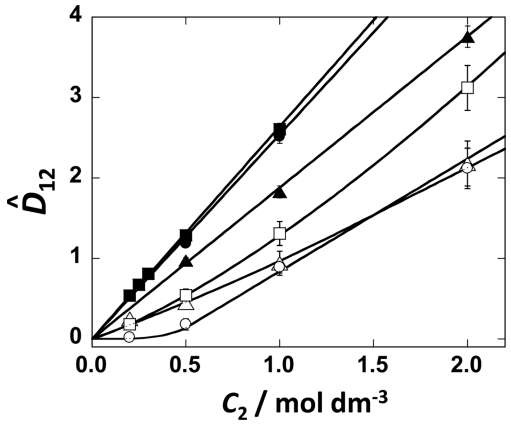

Figure 3. Normalized cross-diffusion coefficient, $\hat{D}_{12}$, as a function of salt concentration, C_2, describing polymer diffusiophoresis for NaSCN (○), KCSCN (□), and NH_4SCN (△) and NaCl (●), KCl (■), and NH_4Cl (▲). For the chloride salts, the solid lines are linear fits through the data. For the thiocyanate salts, solid curves are guides to the eye.

experimental results on the corresponding chloride salts. In all cases, $\hat{D}_{12}$ increases as salt concentration increases and approaches zero as $C_2 \to 0$. At a given salt concentration, the magnitude of $\hat{D}_{12}$ observed for a thiocyanate salt is roughly half that observed for the corresponding chloride salt. Interestingly, the trend $K^+ \approx Na^+ > NH_4^+$ observed in the case of chlorides is not the same as that observed in the case of thiocyanates; in the latter case, only the trend $K^+ > NH_4^+$ is preserved. This finding can mainly be attributed to the distinctive behavior of $\hat{D}_{12}(C_2)$ observed in the case of NaSCN. Specifically, the magnitude of $\hat{D}_{12}$ for this salt is appreciably lower than that observed for the other two thiocyanate salts at low C_2. As salt concentration increases, $\hat{D}_{12}$ increases, reaching values that are approximately equal to those obtained in the case of NH_4SCN. Correspondingly, the $\hat{D}_{12}$ values obtained in the KSCN case remain somewhat higher. The observed behavior of $\hat{D}_{12}(C_2)$ in the NaSCN case can be explained if SCN^- binding on the electrically neutral PEG chains is taken into account. Because of anion binding, PEG chains have an extrinsic negative charge that can interact with electric fields.

The salt concentration gradient responsible for diffusiophoresis generates an internal electrical-potential gradient proportional to $(D_M - D_L)/(D_M + D_L)$,[11,16,29,30] where D_M and D_L are the tracer-diffusion coefficients of the cation (M) and anion (L) respectively. Similarly to electrophoresis, this electrical-potential gradient drives the migration of charged particles. In the presence of anion binding, this mechanism contributes to the net value of $\hat{D}_{12}$.

The electrostatic effects of ion binding on polymer diffusiophoresis are illustrated in Figure 4A,B. If the cation tends to diffuse faster than the anion ($D_M - D_L > 0$), a gradient of electrical potential is generated in the opposite direction of the salt concentration gradient. Thus, a negatively charged particle will diffuse from high to low salt concentration, that is, $\hat{D}_{12} > 0$ (Figure 4A). We deduce that this circumstance occurs in the cases of KSCN and NH_4SCN, for which we calculate $D_M/D_L = 1.10$ for both salts.[27,28,31] On the other hand, if the anion tends to diffuse faster than the cation ($D_M - D_L < 0$), this internal electrical potential is in the same direction as ∇C_2, and a negatively charged particle will diffuse from low to high salt concentration, that is, $\hat{D}_{12} < 0$ (Figure 4B). We deduce that this is the case for NaSCN for which $D_M/D_L = 0.75$.[27,28,31] Based on this electrostatic mechanism, the $\hat{D}_{12}$ curve associated with NaSCN should be located below those associated with the other two thiocyanates. Furthermore, because the relative difference in ionic mobilities is significantly larger for NaSCN (25%) than for the other two salt cases (10%), this electrostatic mechanism is expected to be relatively more important for NaSCN. Our analysis is qualitatively consistent with our experimental results. It is important to remark that cation binding would have predicted the opposite effect, in disagreement with our experimental findings.

We propose the following mechanism of SCN^- binding to PEG: Because of oxygen's electron-withdrawing ability, the two methylene groups in the V-shaped sequence $—CH_2—O—CH_2—$ are expected to have a partial positive charge, giving rise to a local permanent dipole perpendicular to the polymer backbone. Although further studies are needed to characterize how this anion binds to PEG chains, we speculate that binding occurs when S is located near these two methylene groups because (1) the negative charge of thiocyanate is mainly localized on the sulfur atom ($^-S—C{\equiv}N$), (2) N prefers to interact with water molecules by hydrogen bonding, and (3) the distance between the two C atoms of the methylene groups (~2.3 Å) is comparable to the size of the S atom (van der

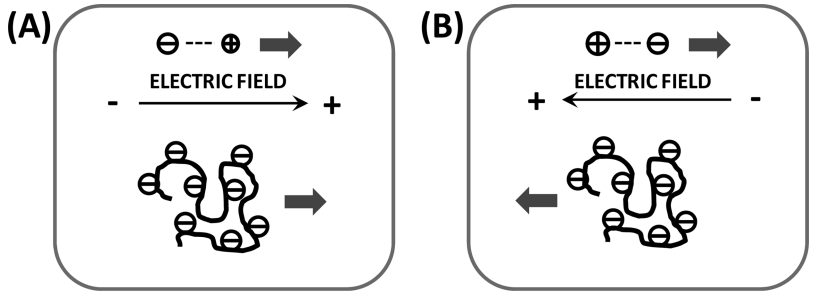

Figure 4. Effects of salt concentration gradients on the migration of a negatively charged polymer coil. In all cases, diffusion of salt ions occurs from left to right; the salt concentration gradient (not shown) points to the left. (A) The cation tends to diffuse faster than the anion, thereby inducing an internal electric field in the same direction as salt diffusion. Diffusiophoresis of negatively charged polymer points to the right ($\hat{D}_{12} > 0$). (B) The anion tends to diffuse faster than the cation, thereby inducing an internal electric field in the direction opposite to that of salt diffusion. Diffusiophoresis of negatively charged polymer points to the left ($\hat{D}_{12} < 0$). Opposite effects will occur for a positively charged polymer.

DOI: 10.1021/la5046223
Langmuir 2015, 31, 1353−1361

Waals radius, 1.8 Å). According to this description, each monomeric unit of PEG is potentially a binding site.

3.3. Theoretical Analysis. To quantitatively examine the effect of anion binding on salt osmotic diffusion and polymer diffusiophoresis, we consider the following relations based on irreversible thermodynamics[11−13]

$$\hat{D}_{12} = \gamma - \lambda \tag{3a}$$

$$\hat{D}_{21} = \gamma + C_2\bar{V}_1 - \alpha\lambda \tag{3b}$$

where $\gamma \equiv \lim_{C_1\to 0}(\mu_{12}/\mu_{22})$ and $\lambda \equiv -\lim_{C_1\to 0}(L_{12}/L_{11})$ are the thermodynamic and transport quantities, respectively; $\mu_{ij} \equiv (\partial\mu_i/\partial C_j)_{C_k,k\neq j}$ represents isothermal and isobaric chemical-potential derivatives, with μ_i being the chemical potential of component i; L_{ij} represents the Onsager transport coefficients in the solvent-fixed frame; and $\alpha \equiv D_1^0/D_2$. Because α is small (2−3%, see Supporting Information) and the magnitude of γ is comparable to that of λ, the contribution of $\alpha\lambda$ in eq 3b is small. This implies that $\hat{D}_{21}$ approximately depends on the thermodynamic quantity γ only. For each salt, the corresponding average value of α is reported in Table 1. In eq 3b, the approximation $C_0\bar{V}_0 = 1 - C_2\bar{V}_2 \approx 1$ has been used, where C_0 is the water molar concentration and $\bar{V}_0 = 0.01807$ dm^3·mol^{-1} is the water molar volume. This approximation gives a maximum error of ∼5% at the highest experimental salt concentrations.

Table 1. Parameters Extracted from $\hat{D}_{12}(C_2)$ and $\hat{D}_{21}(C_2)$

thiocyanate salt	α	$N_w^{(M)}$	K (mol dm^{-3})	N_w^0	$b'_{12}/\bar{V}_0$
NaSCN	0.036	2200	6.4 ± 0.1	−730 ± 30	60 ± 3
KSCN	0.033	2000	6.2 ± 0.1	−890 ± 30	61 ± 4
NH_4SCN	0.033	1700	5.3 ± 0.1	−1360 ± 30	50 ± 4

The thermodynamic quantity γ in eq 3b can be expressed as $\gamma = N_w\bar{V}_0\,C_2$,[13] where N_w is the thermodynamic excess ($N_w > 0$, salting-out) or depletion ($N_w < 0$, salting-in) of water molecules around a polymer coil. Thus, N_w characterizes the nature and strength of polymer−salt net interactions in water. For univalent salts, one can write $N_w = (N_w^{(M)} + N_w^{(L)})/2$ in the case of salting-out interactions, where $N_w^{(M)}$ and $N_w^{(L)}$ are the water thermodynamic excesses defined with respect to hypothetical solutions of only cations (M) and only anions (L), respectively.[32] Both $N_w^{(M)}$ and $N_w^{(L)}$ can be approximately assumed to be constant up to $C_2 \approx 1$ mol·dm^{-3}. For the thiocyanate salts, we modify this expression to explicitly consider anion binding with the reasonable assumption that polymer−ion binding is fast compared to diffusion.

To describe anion binding, we introduce ν_L, the number of anions bound to one polymer chain at equilibrium. The value of ν_L increases with salt concentration (at constant C_1) until it reaches the value of the total number of binding sites, n. The simplest model describing polymer−ligand binding is the Scatchard model

$$\nu_L = \frac{nC_2}{K + C_2} \tag{4}$$

where K is the intrinsic dissociation constant of an isolated site. The Scatchard model assumes that all binding sites on the polymer chain are equivalent and independent. The former assumption is straightforwardly justified by considering that each identical —CH_2—O—CH_2— group on the PEG chain is potentially a binding site. Accordingly, we set $n = 424$ for the PEG sample investigated. The latter assumption represents a limitation of the proposed model due to electrostatic interactions between anions bound to adjacent sites and polymer conformational changes that might locally occur because of the binding process. In eq 4, we have also approximated the thermodynamic activity of the anion with C_2. Because the anion activity coefficient cannot be neglected within the experimental range of salt concentrations, K should be regarded as an apparent concentration-based dissociation constant. Finally, note that the use of the total anion concentration, C_2, in eq 4, in place of the concentration of free anions, which is consistent with the limiting condition of $C_1/C_2 \to 0$, can be easily verified by showing that $\nu_L C_1$ is small compared to C_2 at the experimental polymer concentration. Even considering these limitations, the proposed Scatchard model still represents a valuable description of our experimental results because it describes the following two fundamental aspects of the observed salting-in interactions: ion binding and saturation of binding sites at high salt concentrations.

A relation between γ and ν_L can be obtained by considering the equilibrium-dialysis scheme described in Figure 2. Here, it is convenient to link γ to the partial derivative describing salt partitioning between the two compartments

$$\gamma + \bar{V}_1C_2 = -\left(\frac{\partial C_2}{\partial C_1}\right)_{a_2} \tag{5}$$

where a_2 is the salt thermodynamic activity and the approximation $1 - C_2\bar{V}_2 \approx 1$ has been applied. The ternary compartment in Figure 2 is characterized by the polymer and salt concentrations, C_1 and C_2, respectively, whereas the attached binary compartment is characterized by the salt concentration C_2'. The corresponding mean ionic thermodynamic activity is $a_2 = C_2'f_2$, where $f_2(C_2')$ is the salt mean ionic activity coefficient. To describe the polymer−salt interaction in the ternary compartment, we consider a model based on the existence of two domains. The first domain is represented by the salt−water layers surrounding the macromolecules. This local domain is in chemical equilibrium with the second domain, a bulk domain that represents the remaining salt−water solution in the ternary compartment. At equilibrium, $a_2 = (C_MC_L)^{1/2}f_2$, where C_M and C_L are the bulk-domain concentrations of cations and anions, respectively. If the binary compartment is sufficiently large, a change in C_1 will affect C_2 in the ternary compartment but will not change a_2 and C_2'. The effect of C_1 on C_2 is described by the partitioning property $(\partial C_2/\partial C_1)_{a_2}$ in eq 5 or, equivalently, by $(\partial C_2/\partial C_1)_{C_2'}$. An expression for the partitioning coefficient can be obtained by expressing C_M and C_L as functions of C_1. For the cation, we consider the excluded volume,[11,36] $\bar{V}_1 + N_w^{(M)}\bar{V}_0$, associated with the presence of the local domain, which is depleted in cation concentration because of the volume of the macromolecules themselves ($\bar{V}_1$) and salting-out interactions ($N_w^{(M)}\bar{V}_0$). Thus, the cation concentration in the bulk domain is $C_M = C_2/[1 - (\bar{V}_1 + N_w^{(M)}\bar{V}_0)C_1]$. For the anion, we remove the contribution of bound anions from C_2 and consider the excluded volume associated with the volume of the bare macromolecules. Thus, the anion concentration in the bulk domain is $C_L = (C_2 - \nu_L C_1)/(1 - \bar{V}_1\,C_1)$. Because $C_M > C_L$, this equilibrium-dialysis equilibrium is analogous to the Donnan equilibrium for charged macromolecules,[32] where M and L act as the counterion and co-ion, respectively, of the negatively charged polymer chains.

DOI: 10.1021/la5046223
Langmuir 2015, 31, 1353−1361

As in the case of Donnan equilibrium, we assume that the condition $(C_L C_M)^{1/2} = C_2'$ applies when chemical equilibrium is reached.[32] This condition, which assumes that the mean ionic activity coefficient of the salt in the bulk domain of the ternary component coincides with $f_2(C_2')$, can be rewritten as

$$\ln \frac{C_2'}{C_2} = \frac{1}{2} \ln \frac{1 - (\nu_L/C_2)C_1}{[1 - (\overline{V}_1 + N_w^{(M)}\overline{V}_0)C_1](1 - \overline{V}_1 C_1)} = \left[\overline{V}_1 + \frac{1}{2}\left(N_w^{(M)}\overline{V}_0 - \frac{\nu_L}{C_2}\right)\right]C_1 + ... \quad (6)$$

where the last term on the right-hand side represents the first-order term in C_1, obtained using the series expansion $\ln(1 + x) = x + \cdots$. One can determine $(\partial C_2/\partial C_1)_{C_2'}$ from the differentiation of eq 6 and insert the obtained expression of this partial derivative into eq 5, giving

$$\gamma = \frac{1}{2}\left(N_w^{(M)}\overline{V}_0 - \frac{\nu_L}{C_2}\right)C_2 \quad (7)$$

From eq 7, one can also deduce that the water thermodynamic excess is given by $N_w = [N_w^{(M)} - \nu_L/(\overline{V}_0 C_2)]/2$. Note that, contrary to the salting-out case, N_w cannot be approximated as a constant independent of C_2. According to eq 4, $N_w = [N_w^{(M)} - n/(K\overline{V}_0)]/2$ when $C_2 = 0$ and increases as the salt concentration increases.

To quantitatively describe $\hat{D}_{21}(C_2)$, we substituted $\lambda = \gamma - \hat{D}_{12}$ into eq 3b and determined K by applying the method of least squares to our experimental data up to $C_2 = 1$ mol·dm^{-3} based on the expression $(\hat{D}_{21} - \alpha\hat{D}_{12} - C_2\overline{V}_1)/(1 - \alpha) = N_w^{(M)}\overline{V}_0 - n/(K + C_2)$ with $n = 424$ (number of PEG monomeric units) and estimated values of $N_w^{(M)}$. To obtain reasonable estimates of $N_w^{(M)}$, we considered our previous results on the chloride salts[12] and assumed that the contribution of chloride to the salting-out interaction is zero, consistent with the approximately neutral location of this anion within the Hofmeister series.[5,6] The chosen values of $N_w^{(M)}$ and the corresponding determined values of K are reported in Table 1. Note that approximating eq 3b as $\hat{D}_{21} \approx \gamma + C_2\overline{V}_1$ (i.e., neglecting $\alpha\gamma - \alpha\hat{D}_{12}$) gives the same values of K within the experimental error. Substitution of these K values into eq 5 shows that the fraction of occupied sites increases from $\nu_L/n \approx 3\%$ to $\nu_L/n \approx 25\%$ as C_2 increases from 0.2 to 2 mol·dm^{-3}, with ν_L/n reaching the value of 50% at the hypothetical high salt concentration of $C_2 = K \approx 6$ mol·dm^{-3}. Consistent with this observation, numerical examinations show that $\nu_L C_1$ is less than 2% of C_2, thereby justifying the validity of the approximation $C_L \approx C_2$ in eq 4.

The extracted values of K follow the trend $Na^+ > K^+ > NH_4^+$. However, because the value of K is affected by the choice of $N_w^{(M)}$, this ranking does not necessarily mean that K depends on the cation type, but only that changing the cation has a more significant effect on thiocyanates than on chlorides. To unambiguously characterize the salting-in strengths of the three thiocyanate salts, we report in Table 1 the thermodynamic parameter $N_w^0 \equiv [N_w^{(M)} - n/(K\overline{V}_0)]/2$, namely, N_w at $C_2 = 0$.

We now turn our attention to $\hat{D}_{12}(C_2)$ with the goal of quantitatively examining the electrostatic mechanism discussed in section 3.2. To assess its importance, we formally decompose $\hat{D}_{12}(C_2)$ into two contributions

$$\hat{D}_{12} = \hat{D}_{12}^{el} + \hat{D}_{12}' \quad (8)$$

In eq 8, $\hat{D}_{12}^{el}$ is the electrostatic contribution to diffusiophoresis, and $\hat{D}_{12}'$ is a residual contribution that accounts for polymer–salt specific interactions. Our goal is to theoretically determine $\hat{D}_{12}^{el}(C_2)$ to evaluate $\hat{D}_{12}'(C_2)$ for a more appropriate comparison among the three cation cases and with the corresponding chloride salts. The determination of $\hat{D}_{12}^{el}$ is based on two important approximations that are highlighted alongside the derivation of the $\hat{D}_{12}^{el}$ expression below.

It can be shown[11] that the gradient of the electrical potential, ψ, associated with a salt concentration gradient is

$$\frac{F\nabla\psi}{RT} = (\tau_M y_M - \tau_L y_L)\nabla C_2 \quad (9)$$

where F is the Faraday constant, R is the ideal-gas constant, and T is the temperature. In eq 9, $y_M \equiv 1 + (d \ln f_M)/(d \ln C_M)$ and $y_L \equiv 1 + (d \ln f_L)/(d \ln C_L)$ are the thermodynamic factors associated with the activity coefficients of the individual ions f_M and f_L, respectively, with $f_2 = (f_M f_L)^{1/2}$ and $y_2 = (y_M + y_L)/2$. In addition, $\tau_L = Đ_L/(Đ_L + Đ_M)$ and $\tau_M = Đ_M/(Đ_L + Đ_M)$ are the transfer numbers of the anion and cation, respectively (with $\tau_L + \tau_M = 1$), and $Đ_L$ and $Đ_M$ are the corresponding Stefan–Maxwell diffusion coefficients describing the frictional interactions of the two ions with water.[37] These coincide with the corresponding tracer-diffusion coefficients, $Đ_L = D_L$ and $Đ_M = D_M$, in the limit of $C_2 \to 0$. Equation 9 requires the knowledge of unavailable transfer numbers and activity coefficients of individual ions in water. However, if $y_M = y_L$ and $Đ_L/Đ_M$ is independent of salt concentration, eq 9 can be rewritten as

$$\frac{F\nabla\psi}{RT} = \frac{D_L - D_M}{D_L + D_M}\frac{y_2\nabla C_2}{C_2} \quad (10)$$

This equation is expected to be a good approximation when C_2 is low and Debye–Hückel effects dominate the behavior of the thermodynamic and transport properties of binary salt–water systems. However, appreciable deviations of eq 10 from eq 9 can occur as salt concentration increases. The application of eq 10 instead of eq 9, which enables the use of the available tracer-diffusion coefficients of ions, represents the first important approximation toward the determination of $\hat{D}_{12}^{el}$.

As in the case of electrophoresis, we consider the effect of $\nabla\psi$ on the molar flux of charged polymer chains (P) with k anions (L) bound to them, PL_k. Specifically, we write

$$-J_{PL_k}^{el} = C_{PL_k} D_{PL_k} \frac{(-k)\varepsilon_{PL_k} F\nabla\psi}{RT} \quad \text{with } k = 0, 1, 2, ..., n \quad (11)$$

where $J_{PL_k}^{el}$, C_{PL_k}, and D_{PL_k} are the molar flux, molar concentration, and tracer-diffusion coefficient, respectively, of PL_k. In eq 11, one should reasonably assume that the binding of relatively small ions has a relatively small effect on the polymer hydrodynamic radius compared to the experimental error. This implies that tracer diffusion of any PL_k species can be set to be equal to D_1^0. The factor $-k$ represents the electrical charge of PL_k, and ε_{PL_k} is an electrostatic shielding coefficient. Note that $\varepsilon_{PL_k} = 1$ in the limit of $C_2 \to 0$ and sharply decreases as the ionic strength increases;[11] ε_{PL_k} also depends on the size of the particle and other structural properties in general. To obtain an expression for $\hat{D}_{12}^{el}$, we consider the total molar flux of the

DOI: 10.1021/la5046223
Langmuir 2015, 31, 1353–1361

polymer component, $J_1^{el} = \sum_{k=0}^{n} J_{PL_k}^{el}$, driven by this electrostatic mechanism

$$\frac{-J_1^{el}}{\nabla C_2} = (-\varepsilon\nu_L)\frac{D_L - D_M}{D_L + D_M}\frac{C_1 D_1^0 y_2}{C_2} \quad (12)$$

where we have also used eq 10 and the definitions $\nu_L \equiv \sum_{k=0}^{n} kC_{PL_k}/C_1$ and $\varepsilon \equiv (\sum_{k=0}^{n} kC_{PL_k}\varepsilon_{PL_k})/(\sum_{k=0}^{n} kC_{PL_k})$. The right-hand side of eq 12 is the polymer cross-diffusion coefficient according to eq 1a, with $C_1 D_1^0 y_2/C_2$ being a normalization factor in eq 2a. By considering eq 2a and observing that the reference-frame term is associated with $\hat{D}'_{12}$, one can deduce that

$$\hat{D}_{12}^{el} = \frac{\varepsilon\nu_L}{2}\frac{D_M - D_L}{D_M + D_L} \quad (13)$$

It is interesting to observe that eq 13 appears to be identical to the equation derived for particles with an intrinsic charge of Z_P (e.g., proteins) provided that ν_L is replaced by the magnitude of the particle charge, $|Z_P|$, with M and L acting as the particle counterion and co-ion, respectively. However, in contrast to $|Z_P|$, ν_L vanishes as the salt concentration approaches zero (see eq 4). Furthermore, some substantial differences become evident when $\hat{D}_{12}^{el}$ is broken down into its thermodynamic, γ^{el}, and transport, λ^{el}, components ($\hat{D}_{12}^{el} = \gamma^{el} - \lambda^{el}$ from eq 3a). Derivations of expressions for γ^{el} and λ^{el} are reported in the Supporting Information. It can be shown that anion binding leads to $\gamma^{el} = -\nu_L/2 < 0$, consistent with eq 7. This is the opposite of the Donnan-equilibrium result, $\gamma^{el} = |Z_P|/2 > 0$, obtained for particles with an intrinsic charge.[11] The difference in γ^{el} between the two cases can be explained by considering that the addition of a neutral particle acts as sink for the binding anions, thereby leading to a reduction of the salt chemical potential ($\gamma^{el} < 0$). On the other hand, the addition of charged particles is accompanied by the addition of counterions, thereby leading to an increase in the salt chemical potential due to the common-ion effect ($\gamma^{el} > 0$). In relation to the transport quantity, the difference can be easily appreciated by deriving the corresponding expression in the limit of $\varepsilon = 1$ (i.e., $C_2 \to 0$ with $C_1/C_2 \to 0$). In this case, it can be shown that $\lambda^{el} = -\nu_L\tau_M$ for extrinsically charged particles is not the same as $\lambda^{el} = |Z_P|\tau_L$ for intrinsically charged particles, which is extracted from the Nernst–Hartley equations.[9]

To evaluate ε, we use $\varepsilon = f(\kappa R_P)/(1 + \kappa R_P)$, where $f(\kappa R_P)$ is the Henry function with $f(0) = 1$ (Debye–Hückel limit) and $f(\infty) = {}^3/_2$ (Smoluchowski limit); $\kappa \equiv (8000\pi N_A \lambda_B I)^{1/2}$ is the Debye constant, where N_A is Avogadro's number, $\lambda_B = 0.7151$ nm is the Bjerrum length for water at 298.15 K, and I is the solution ionic strength (C_2 in our case); and R_P is the radius of the particle assumed to be spherical.[11,38,39] In our case, we used $R_P = 4.46$ nm as the equivalent hydrodynamic radius of PEG extracted by applying the Stokes–Einstein equation for spheres to D_1^0.[10] Note that the assumption that R_P (and D_1^0) is the same for all PL_k species implies that $\varepsilon_{PL_k} = \varepsilon$, independent of k.

The proposed expression for ε has been derived for charged impenetrable spheres and represents the second important approximation toward the determination of $\hat{D}_{12}^{el}$. It is important to note that a more general model for the electrophoretic mobility of spherical penetrable particles (applicable to polyelectrolytes) has been developed.[40] This model, which contains a parameter (Debye–Bueche ratio) describing particle penetrability, appears to be potentially more accurate for polymer coils. However, specific macromolecule–salt interactions in water, responsible for preferential binding and preferential exclusion of ions from the aqueous local domain of macromolecules, are not taken into account. For instance, PEG chains, which are penetrable to the neutral water molecules, can be regarded as impenetrable to sodium ions due to salting-out interactions. This is a critical property of our systems and undermines the application of the other model. Thus, we chose the model for charged impenetrable spheres because of its relative simplicity and internal consistency. Moreover, we believe that this model is sufficiently adequate for the examination of polymer diffusiophoresis because our main goal was an internal comparison among three homologous polymer–salt–water systems that differ only in the nature of the cation.

The calculated values of ε are reported in Table 2, together with the corresponding values of κR_P and $f(\kappa R_P)$. To calculate

Table 2. Parameters Extracted from Ternary Diffusion Coefficients (R_P = 4.46 nm)

C_2 (mol dm^{-3})	κR_P	$f(\kappa R_P)$	ε
0.2	6.55	1.20	0.158
0.5	10.36	1.26	0.111
1.0	14.66	1.30	0.083
2.0	20.73	1.34	0.062

$\nu_L(C_2)$ in eq 13, we used the K values in Table 1 with n = 424. Our $\hat{D}_{12}^{el}$ (C_2) results are shown in Figure 5. For KSCN, the

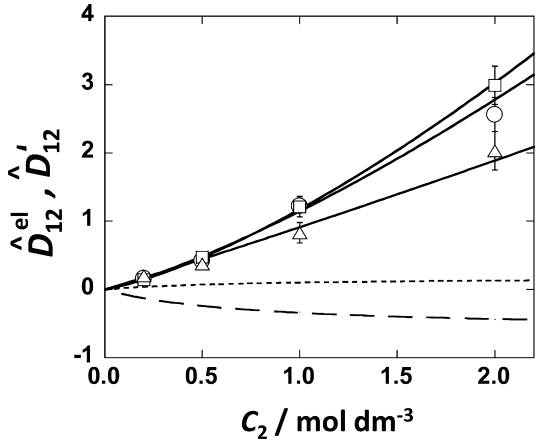

Figure 5. Residual normalized cross-diffusion coefficient, $\hat{D}'_{12}$, as a function of salt concentration, C_2, describing polymer diffusiophoresis for NaSCN (○), KCSCN (□), and NH_4SCN (△). Solid curves are guides to the eye. The dotted and dashed curves represents the theoretical calculation of $\hat{D}_{12}^{el}$ for KSCN and NaSCN, respectively.

$\hat{D}_{12}^{el}(C_2)$ values are slightly positive; those related to NH_4SCN are essentially the same and were omitted for clarity. Because of differences in tracer-diffusion coefficients (see section 3.2), the $\hat{D}_{12}^{el}(C_2)$ values in the case of NaSCN are negative with a relatively large magnitude when compared with those of the other two salt cases.

In Figure 5, we also show the $\hat{D}'_{12}(C_2)$ curves, obtained by subtracting the $\hat{D}_{12}^{el}$ contribution from $\hat{D}_{12}$. These curves follow the order $K^+ \approx Na^+ > NH_4^+$, which is the same as that observed for the chloride salts. To characterize the magnitude of $\hat{D}'_{12}(C_2)$, we applied the weighted linear least-squares method to our data to determine the slope, b_{12}, based on $\hat{D}'_{12}(C_2) = b_{12}C_2$. The values of $b_{12}/\bar{V}_0$, which are reported in Table 1, show that $b_{12}/$

DOI: 10.1021/la5046223
Langmuir 2015, 31, 1353–1361

$\bar{V}_0 \approx 60$ for NaSCN and KSCN, whereas the value obtained for NH_4SCN is 20% lower. These results can be compared with those previously obtained by applying $\hat{D}_{12}(C_2) = b_{12}\, C_2$ to the corresponding chloride curves in Figure 3: $b_{12}/\bar{V}_0 \approx 140$ for NaCl and KCl, with the value obtained for NH_4Cl being 30% lower.[13] Thus, if anion binding is taken into account, the cation ranking for thiocyanate salts closely follows the ranking previously observed for chloride salts.

4. CONCLUSIONS

The behavior of macromolecule diffusiophoresis, $\hat{D}_{12}(C_2)$, and salt osmotic diffusiophoresis, $\hat{D}_{21}(C_2)$, can be used to probe salting-in interactions. Whereas $\hat{D}_{12}(C_2)$ reflects the mechanism of macromolecule−salt interactions (i.e., anion binding), $\hat{D}_{21}(C_2)$ can be used to quantitatively characterize the magnitude of thermodynamic interactions.

■ ASSOCIATED CONTENT

Supporting Information

Tables reporting ternary diffusion coefficients and physicochemical properties of aqueous salts (section S1), thermodynamic relations based on the Scatchard model (section S2), and a theoretical examination of anion binding based on irreversible thermodynamics (section S3). This material is available free of charge via the Internet at http://pubs.acs.org.

■ AUTHOR INFORMATION

Corresponding Author

*Phone: (817) 257-6215. Fax: (817) 257-5851. E-mail: O.Annunziata@tcu.edu.

Notes

The authors declare no competing financial interest.

■ ACKNOWLEDGMENTS

This work was supported by the ACS Petroleum Research Fund (47244-G4) and TCU Research and Creative Activity Funds.

■ REFERENCES

(1) Collins, K. D.; Washabaugh, M. W. The Hofmeister effect and the behaviour of water at interfaces. *Q. Rev. Biophys.* **1985**, *18*, 323−422.

(2) Cacace, M. G.; Landau, E. M.; Ramsden, J. J. The Hofmeister series: Salt and solvent effects on interfacial phenomena. *Q. Rev. Biophys.* **1997**, *30*, 241−277.

(3) Zhang, Y. J.; Furyk, S.; Sagle, L. B.; Cho, Y.; Bergbreiter, D. E.; Cremer, P. S. Effects of Hofmeister Anions on the LCST of PNIPAM as a Function of Molecular Weight. *J. Phys. Chem. C* **2007**, *111*, 8916−8924.

(4) Okur, H. I.; Kherb, J.; Cremer, P. S. Cations Bind Only Weakly to Amides in Aqueous Solutions. *J. Am. Chem. Soc.* **2013**, *135*, 5062−5067.

(5) Zhang, Y. J.; Cremer, P. S. Interactions between macromolecules and ions: The Hofmeister series. *Curr. Opin. Chem. Biol.* **2006**, *10*, 658−663.

(6) Zhang, Y. J.; Cremer, P. S. Chemistry of Hofmeister Anions and Osmolytes. *Annu. Rev. Phys. Chem.* **2010**, *61*, 63−83.

(7) Ninham, B. W.; Yaminsky, V. Ion Binding and Ion Specificity: The Hofmeister Effect and Onsager and Lifshitz Theories. *Langmuir* **1997**, *19*, 2097−2018.

(8) Salis, A.; Ninham, B. W. Models and mechanisms of Hofmeister effects in electrolyte solutions, and colloid and protein systems revisited. *Chem. Soc. Rev.* **2014**, *43*, 7358−7377.

(9) Gibb, C. L. D.; Gibb, B. C. Anion Binding to Hydrophobic Concavity Is Central to the Salting-in Effects of Hofmeister Chaotropes. *J. Am. Chem. Soc.* **2011**, *133*, 7344−7347.

(10) Rembert, K. B.; Paterová, J.; Heyda, J.; Hilty, C.; Jungwirth, P.; Cremer, P. S. Molecular Mechanisms of Ion-Specific Effects on Proteins. *J. Am. Chem. Soc.* **2012**, *134*, 10039−10046.

(11) Annunziata, O.; Buzatu, D.; Albright, J. G. Protein diffusiophoresis and salt osmotic diffusion in aqueous solutions. *J. Phys. Chem. B* **2012**, *116*, 12694−12705.

(12) McAfee, M. S.; Annunziata, O. Effect of Particle Size on Salt-Induced Diffusiophoresis Compared to Brownian Mobility. *Langmuir* **2014**, *30*, 4916−4923.

(13) McAfee, M. S.; Zhang, H.; Annunziata, O. Amplification of salt-induced polymer diffusiophoresis by increasing salting-out strength. *Langmuir* **2014**, *30*, 12210−12219.

(14) Tyrrell, H. J. V.; Harris, K. R. *Diffusion in Liquids*; Butterworths: London, 1984.

(15) Prieve, D.C. Migration of a colloidal particle in a gradient of electrolyte concentration. *Adv. Colloid Interface Sci.* **1982**, *16*, 321−335.

(16) Keh, H. J.; Anderson, J. L. Colloid transport by interfacial forces. *Annu. Rev. Fluid Mech.* **1989**, *21*, 61−99.

(17) Abécassis, B.; Cottin-Bizonne, C.; Ybert, C.; Ajdari, A.; Bocquet, L. Boosting migration of large particles by solute contrasts. *Nat. Mater.* **2008**, *7*, 785−789.

(18) Prieve, D.C. Particle transport: Salt and migrate. *Nat. Mater.* **2008**, *7*, 769−770.

(19) Palacci, J.; Abécassis, B.; Cottin-Bizonne, C.; Ybert, C.; Bocquet, L. Colloidal Motility and Pattern Formation under Rectified Diffusiophoresis. *Phys. Rev. Lett.* **2010**, *104*, 138302.

(20) Albertsson, P. A. *Partition of Cell Particles and Macromolecules*; Wiley: New York, 1986.

(21) Lin, C. C.; Anseth, K. S. PEG hydrogels for the controlled release of biomolecules in regenerative medicine. *Pharm. Res.* **2009**, *26*, 631−643.

(22) Annunziata, O.; Buzatu, D.; Albright, J. G. Protein Diffusion Coefficients Determined by Macroscopic-Gradient Rayleigh Interferometry and Dynamic Light Scattering. *Langmuir* **2005**, *21*, 12085−12089.

(23) Miller, D. G.; Albright, J. G. Optical methods. In *Measurement of the Transport Properties of Fluids: Experimental Thermodynamics*; Wakeham, W. A., Nagashima, A., Sengers, J. V., Eds.; Blackwell Scientific Publications: Oxford, U.K., 1991; Vol. *III*, pp 272−294.

(24) Miller, D. G.; Vitagliano, V.; Sartorio, R. Some comments on multicomponent diffusion: Negative main term diffusion coefficients, second law constraints, solvent choices, and reference frame transformations. *J. Phys. Chem.* **1986**, *90*, 1509−1519.

(25) Miller, D. G. A Method for Obtaining Multicomponent Diffusion Coefficients Directly from Rayleigh and Gouy Fringe Position Data. *J. Phys. Chem.* **1988**, *92*, 4222−4226.

(26) Zhang, H.; Annunziata, O. Effect of macromolecular polydispersity on diffusion coefficients measured by Rayleigh interferometry. *J. Phys. Chem. B* **2008**, *112*, 3633−3643.

(27) Lobo, V. M. M.; Quaresma, J. L. *Handbook of Electrolyte Solutions*; Elsevier: Amsterdam, 1989.

(28) Mitchell, J. P.; Butler, J. B.; Albright, J. G. Measurement of mutual diffusion coefficients, densities, viscosities, and osmotic coefficients for the system KSCN-H_2O at 25°C. *J. Solution Chem.* **1992**, *21*, 1115−1129.

(29) Gosting, L. J. Measurement and interpretation of diffusion coefficients of proteins. *Adv. Prot. Chem.* **1956**, *11*, 429−554.

(30) Leaist, D.G. The role of supporting electrolytes in protein diffusion. *J. Phys. Chem.* **1989**, *93*, 474−479.

(31) Robinson, R. A.; Stokes, R. H. *Electrolyte Solutions*; Dover: Mineola, MN, 2002.

(32) Record, M.T.; Anderson, C.F. Interpretation of preferential interaction coefficients of nonelectrolytes and of electrolyte ions in terms of a two domain model. *Biophys. J.* **1995**, *68*, 786−794.

DOI: 10.1021/la5046223
Langmuir 2015, 31, 1353−1361

(33) van Holde, K.E.; Johnson, C.; Ho, P.S. *Principles of Physical Biochemistry*; Prentice-Hall: Upper Saddle River, NJ, 1998.
(34) Timasheff, S.N. Protein hydration, thermodynamic binding, and preferential hydration. *Biochemistry* **2002**, *41*, 13473−13482.
(35) Parsegian, V. A.; Rand, R. P.; Rau, D. C. Osmotic stress, crowding, preferential hydration, and binding: A comparison of perspectives. *Proc. Natl. Acad. Sci. U.S.A.* **2000**, *97*, 3987−3992.
(36) Vergara, A.; Paduano, L.; Mangiapia, G.; Sartorio, R. Diffusion Coefficient Matrix in Nonionic Polymer−Solvent Mixtures. *J. Phys. Chem. B* **2001**, *105*, 11044−11051.
(37) Krishna, R. Diffusion in Multicomponent Electrolyte Systems. *Chem. Eng. J.* **1987**, *35*, 19−24.
(38) Carbeck, J. D.; Negin, R. S. Measuring the size and charge of proteins using protein charge ladders, capillary electrophoresis, and electrokinetic models of colloids. *J. Am. Chem. Soc.* **2001**, *123*, 1252−253.
(39) Henry, D.C. The Cataphoresis of Suspended Particles. Part I. The Equation of Cataphoresis. *Proc. R. Soc. London A* **1931**, *133*, 106−129.
(40) Fujita, H. Notes on the Calculation of Electrophoresis of Polyelectrolytes with Partial Free Drainage. *J. Phys. Soc. Jpn.* **1957**, *8*, 968−973.

DOI: 10.1021/la5046223
Langmuir 2015, 31, 1353−1361